Examining the Impact of Polyzwitterion Chemistry on Lithium Ion Transport in Ionogel Electrolytes

Morgan E. Taylor,[1] David Clarkson,[2] Steven G. Greenbaum,[2] and Matthew J. Panzer,[1]*

[1]Department of Chemical & Biological Engineering

Tufts University

4 Colby Street, Medford, MA 02155, USA

[2]Department of Physics and Astronomy

Hunter College of CUNY

695 Park Avenue, New York, NY 10065, USA

***Corresponding Author**

<u>Email</u>: matthew.panzer@tufts.edu

ABSTRACT

A series of polyzwitterion-supported gels featuring two classes of lithium-containing ionic liquid (IL) electrolytes has been created in order to examine the impact of different zwitterionic (ZI) group chemistries on lithium ion conductivity in these nonvolatile electrolytes. ZI homopolymer-supported gels containing poly(carboxybetaine methacrylate) (pCBMA), poly(2-methacryloyloxyethyl phosphorylcholine) (pMPC), poly(sulfobetaine vinylimidazole) (pSBVI), and poly(sulfobetaine 2-vinylpyridine) (pSB2VP) were realized by rapid, *in situ* UV photopolymerization. Within a 1M solution of lithium bis(trifluoromethylsulfonyl)imide (LiTFSI) in a conventional IL, strong Coulombic interactions between ZI moieties and Li^+ cations promoted higher ion self-diffusivities for all zwitterion types and generated improved Li^+ conductivities. In particular, the pCBMA and pMPC gels exhibited improved lithium transference numbers of 0.37 and 0.38, respectively, compared to 0.23 for the IL solution. In the solvate ionic liquid (SIL) prepared from an equimolar mixture of LiTFSI and tetraglyme, the pCBMA scaffold resulted in the largest room temperature Li^+ conductivity achieved, 0.44 mS cm^{-1} (versus 0.23 mS cm^{-1} in the neat SIL). The carboxybetaine ZI motif yielded the largest boost in Li^+ conductivity in both IL electrolyte types, which was found to be correlated with this monomer generating the largest downfield ^{7}Li NMR chemical shift in solution. This study illustrates the great potential of polyzwitterions for future application in lithium-ion batteries and reveals the importance of zwitterion chemistry when selecting materials for nonaqueous ionogel electrolytes.

Keywords: Gel electrolyte, zwitterion, lithium-ion, enhanced transport, ionic liquid, ion diffusion

INTRODUCTION

In the world of consumer electronics, lithium-ion batteries (LIBs) are the most ubiquitous option for rechargeable energy storage due to a high energy density and low self-discharge.[1,2] However, despite their widespread use, there is considerable research ongoing to further improve the properties of LIBs, such as energy density, safety, lifespan, and charging speed, to name a few.[3,4] Improving battery safety through careful design of the electrolyte is one area of focus, and a common strategy that has been utilized is the dissolution of a lithium salt in an ionic liquid (IL) to form a nonvolatile LIB electrolyte. ILs are molten salts at or near ambient temperature that consist of weakly-coordinated cations and anions. Due to their many advantageous properties, including: ultralow volatility, high thermal stability, and moderate ionic conductivity (~0.1-20 mS cm^{-1}) ILs have been well-studied in the field of electrochemical energy storage.[5,6] Additionally, owing to a wide electrochemical stability window (~3-5 V), certain ILs may be well-suited for use as safer LIB electrolytes.[7,8]

When discussing IL-based LIB electrolytes, it is also worth mentioning a subclass of ILs known as *solvate* ionic liquids (SILs). SILs are prepared by combining a salt with a strongly coordinating ligand to form an ion complex with either the cation or anion.[9] Glymes, such as tetra(ethylene glycol) dimethyl ether (tetraglyme, G4), have been known to dissolve lithium salts at high concentrations, and there are numerous studies that report the preparation of SILs along with their use in electrochemical energy storage applications.[10,11] When combined with lithium bis(trifluoromethylsulfonyl)imide (LiTFSI) in an equimolar ratio, each tetraglyme molecule forms a stable complex cation with Li^+ to yield a SIL, [Li(G4)][TFSI].[12,13] SILs demonstrate similar properties to conventional ILs, including ultralow vapor pressure and nonflammability, but represent a lower cost alternative as they do not require a difficult synthesis or purification to prepare.[14]

While ILs offer significant improvements to LIB safety when compared to conventional organic electrolytes due to their ultralow volatility and nonflammable nature, there still remains the possibility of leakage when using a liquid electrolyte. To further enhance electrolyte safety, there have been many studies on immobilizing an IL electrolyte with a solid support matrix, such as a polymeric or inorganic nanoparticle-based scaffold, to create what is referred to as an ionogel (or ion gel).[15–19] Polymeric scaffolds are a popular choice for ionogels because through careful selection of the polymer chemistry, desired gel properties can be finely tuned and gel stability can be enhanced.[20–22] In the context of lithium-containing electrolytes, scaffolds containing poly(ethylene oxide) (PEO) or poly(vinylidene fluoride-co-hexafluoropropylene) (PVdF-HFP) have largely been the focus in previous studies that aimed to improve ionogel properties such as stability, lithium transport, and mechanical character.[23–26]

A recently emerging class of scaffold materials that has been of particular interest is polyzwitterions, polymers which bear functional repeat units that each contain an equal number of positively- and negatively-charged groups.[27,28] Zwitterionic (ZI) groups are overall charge neutral, but can exhibit large dipole moments.[29,30] This results in strong Coulombic ZI interactions with ions as well as ZI self-associations, particularly in aqueous environments. ZI groups have been utilized in polymer-supported hydrogels because they can form noncovalent dipole-dipole cross-links that significantly increase gel mechanical properties.[31,32] Zwitterions have also seen use in the field of electrochemical energy storage, and a notable work is the study by Byrne *et al.*, which showed that interactions between ZI additives and lithium salts within an IL electrolyte led to enhanced ionic conductivities.[33] The authors hypothesized that this observation could be related to increased dissociation of the lithium salt due to zwitterion/Li^+ interactions. Reports by the Ohno group demonstrated solubilization of a lithium salt due to strong coordination with zwitterions and also examined the effect of variations in zwitterion chemistry.[34–36] Despite their strong Coulombic interactions with lithium salts and potential benefits for ion-rich systems, as well as the growing use of polyzwitterions for hydrogel scaffolds, ZI (co)polymers for IL-containing electrolytes remain largely unstudied. It was only a few years ago that our group reported the first example of an ionogel electrolyte featuring a ZI copolymer scaffold, wherein we demonstrated not only the effectiveness of ZI cross-links to tune gel mechanical properties, but also the benefit of improved ion dissociation within a hydrophobic IL.[37] In more recent studies, we utilized two different ZI monomers, 2-methacryloyloxyethyl phosphorylcholine (MPC) and sulfobetaine vinylimidazole (SBVI), together to form fully-ZI copolymers in conventional ILs as well as a SIL, and found that ion transport and ionogel mechanical properties varied substantially, depending on the type of IL and the relative amounts of the two ZI groups present in the system.[38–41]

These initial works have demonstrated the promising potential of fully-ZI copolymer scaffolds for ionogel electrolytes that result from a balance between ion-ZI dipole and ZI dipole-dipole interactions, but many unanswered questions still remain. Our studies to date have all focused on the same two ZI monomers, and we have only begun to understand the behaviors of different ZI group chemistries within various types of ILs. Particularly for IL-based electrolytes containing Li^+ ions, with potential for future LIB applications, there is still much work to be done in order to decipher the nature of specific zwitterion/ion interactions and how these impact ion transport. Previous modeling studies performed by the Jiang group compared carboxybetaine (CB) and sulfobetaine (SB) zwitterion moieties and determined their relative interactions with several cations, but these were considered in aqueous environments, and it is unclear if the same trends would be observed in an IL.[42–44] Thus, there is a need to gain a better understanding of how ZI group chemistry influences the properties of an ionogel electrolyte by studying the relative interactions between ions and different ZI groups in nonaqueous, ion-dense environments. In doing so, we aim to promote the design of safer, more efficient electrolytes for energy storage applications through the deliberate choice of both the zwitterion and IL chemistries.

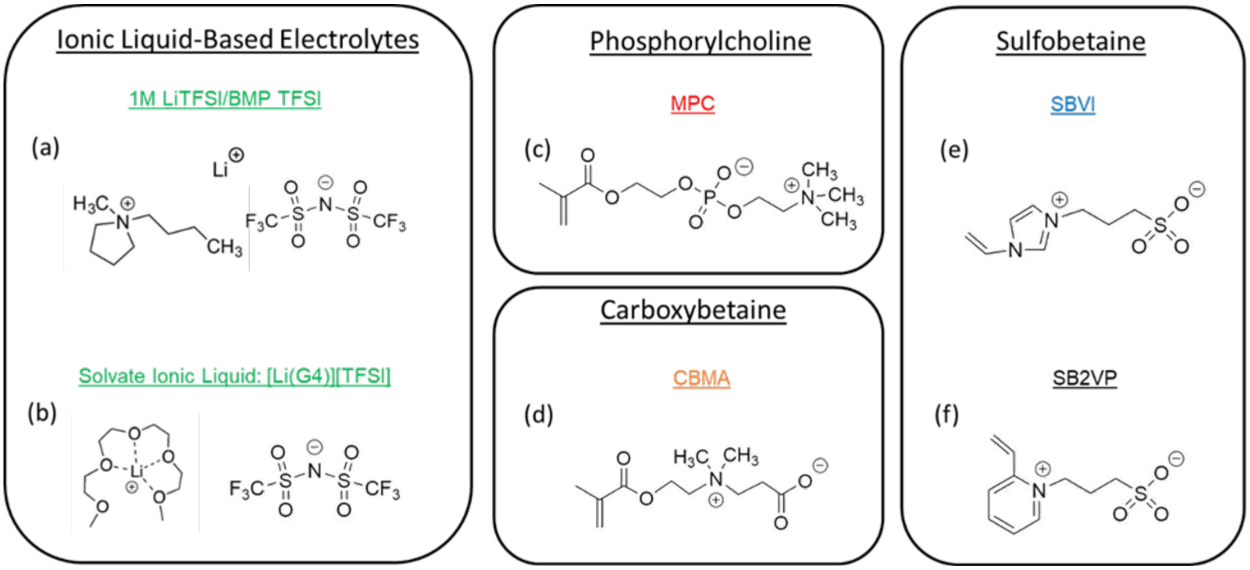

Figure 1. Molecular structures of IL-based electrolyte components: (a) 1M LiTFSI in N-butyl-N-methylimidazolium bis(trifluoromethylsulfonyl)imide (BMP TFSI), (b) solvate ionic liquid, [Li(G4)][TFSI]. Molecular structures of zwitterionic (ZI) monomers employed in this study: (c) MPC, (d) CBMA (carboxybetaine methacrylate), (e) SBVI, and (f) SB2VP (sulfobetaine 2-vinylpyridine).

In this study, we systematically examine how four different ZI homopolymer chemistries (covering the three major zwitterion groups: CB, SB, and phosphorylcholine (PC)) impact ion transport within ionogels featuring two classes of lithium-containing IL electrolytes (a conventional IL/lithium salt solution versus a SIL). The chemical structures of the two electrolytes and four ZI monomers employed are shown in Figure 1. Polyzwitterions formed in the 1M LiTFSI/BMP TFSI electrolyte demonstrated notable Coulombic interactions between all four ZI moieties and the ions present. DC polarization and impedance spectroscopy measurements revealed that significant zwitterion/ion interactions led to an effective improvement of both total ionic conductivity and Li^+ conductivity in this system. This corresponded with greater apparent self-diffusivities of all ions within the ionogels. In the SIL electrolyte, however, ion self-diffusivities were reduced by the presence of the SB and PC polyzwitterions compared to those in the neat SIL, while the CB polyzwitterion scaffold (pCBMA) once again improved ion mobility. In both types of IL environments, the presence of pCBMA promoted the largest increase in room temperature Li^+ conductivity out of all four polyzwitterions examined here. This work illuminates clear differences between the effects of SB, PC, and CB polyzwitterion chemistries on Li^+ transport in IL environments, and, to our knowledge, it represents the first time that a CB polyzwitterion has been examined in a lithium-containing IL, which has revealed its outstanding potential among various ZI groups to enhance Li^+ motion within nonaqueous ionogel electrolytes.

EXPERIMENTAL METHODS

Materials

N-butyl-N-methylpyrrolidinium bis(trifluoromethylsulfonyl)imide (BMP TFSI) (High Purity grade), lithium bis(trifluoromethylsulfonyl)imide (LiTFSI), 2-hydroxy-2-methylpropiophenone (HOMPP), and tetra(ethylene glycol) dimethyl ether (tetraglyme, G4), were purchased from MilliporeSigma and stored in a N_2-filled glove box (H_2O, O_2 <1 ppm). Synthesis reagents, 2-(dimethylamino)ethyl methacrylate (DMAEMA), β-propiolactone (grade II), anhydrous THF, and diethyl ether were purchased from Sigma Aldrich and stored below room temperature until use. Lithium foil (99.9%, 0.75 mm thick) was purchased from Alfa Aesar and stored in an Ar-filled glove box (H_2O, O_2 <0.5 ppm) until preparation of coin cells. The monomer 2-methacryloyloxyethyl phosphorylcholine (MPC) was purchased from Sigma Aldrich (97% purity) and stored in a refrigerator until time of sample preparation. The monomers sulfobetaine vinylimidazole (SBVI) and sulfobetaine 2-vinylpyridine (SB2VP) were prepared according to procedures outlined in previous reports,[37,45] and then stored in the same fashion as MPC. The monomer carboxybetaine methacrylate (CBMA) was synthesized according to the procedure outlined below and the monomer was stored in the refrigerator until time of sample preparation. Celgard separator (25 μm thickness) and stainless steel (SS) coin cell parts (CR2032) were purchased from MTI Corp.

Synthesis of CBMA

CBMA monomer was synthesized following a similar procedure outlined by Zhang *et al.* by reacting DMAEMA and β-propiolactone.[46] First, DMAEMA was dissolved in anhydrous THF and then β-propiolactone was dissolved in anhydrous THF and added dropwise to the solution. The solution was stirred under nitrogen protection at 15 °C for 5 hours and a white precipitate formed. The reaction product was then removed and rinsed first in anhydrous THF and then in diethyl ether to remove leftover reactants. The final product was dried under reduced pressure at room temperature and stored in a refrigerator until use. NMR spectroscopy was performed in a Bruker AVANCE III 500 MHz NMR spectrometer using D_2O as the solvent. ^1H NMR (D_2O, 500 MHz): 6.06 (=CH), 5.68 (=CH), 4.55 (OCH_2), 3.70 (CH_2N), 3.59 (NCH_2), 3.10 (NCH_3), 2.64 (CH_2COO), 1.84 (=CCH_3). See Figure S1 (Supporting Information) for the ^1H NMR spectrum and peak assignments.

Preparation of Lithium-containing Ionic Liquid Electrolytes and Ionogels

A conventional IL/lithium salt solution electrolyte was prepared by dissolving LiTFSI in BMP TFSI at a concentration of 1M and stirring at 50 °C overnight in a N_2-filled glovebox until a homogeneous solution was obtained. A solvate ionic liquid (SIL), [Li(G4)][TFSI], was prepared by combining LiTFSI and tetraglyme (G4) in an equimolar ratio and stirring in a vial at 50 °C in a N_2-filled glovebox until a clear solution was obtained (it should be noted that the final LiTFSI concentration in the resulting SIL is approximately 2.8M). Following its preparation, the SIL was dried over molecular sieve beads (5 Å, Sigma Aldrich) for at least 48 hours before use. Monomer solutions were prepared by adding a ZI monomer at the desired ZI unit:Li^+ ratio and stirring overnight until a clear solution was obtained. ZI unit:Li^+ molar ratios ranging from 1:4 to 2:3, corresponding to ZI unit/(ZI unit + Li^+) mole fractions of 0.2-0.4, were employed in the 1M LiTFSI/BMP TFSI electrolyte (*i.e.* ZI unit concentrations of 0.25-0.67M). ZI unit:Li^+ molar ratios ranging from 1:9 to 1:4, corresponding to ZI unit/(ZI unit + Li^+) mole fractions of 0.1-0.2 (*i.e.* ZI unit concentrations of 0.31-0.70M), were employed in the SIL electrolyte due to its higher Li^+

concentration. For clarity, the ZI unit:Li^+ mole fraction values are used to label the experimental data. To prepare an ionogel, HOMPP photoinitiator (2 wt% monomer basis) was added to a monomer solution, which was stirred for 10 minutes before polymerization was achieved via UV irradiation at 365 nm using a handheld lamp (Spectronic Corp., 8 W) for 10 minutes. Ionogel samples were stored in the glovebox overnight before use.

Preparation of Coin Cells

Coin cells for DC polarization measurements were prepared by loading a liquid electrolyte into or polymerizing an ionogel within pores of the Celgard separator, in order to standardize the geometry and thickness of the cell electrolyte layer. Electrolyte solutions were infiltrated within Celgard separators (17 mm diameter and 25 μm thickness) under mild vacuum conditions for at least 2 hours (prior to UV irradiation, in the case of ionogel precursor solutions). Li|electrolyte|Li coin cells were assembled inside an Ar-filled glovebox and discs of Li^+ metal (~15 mm diameter) were rolled with a glass vial to brighten the lithium metal surface prior to use. For determination of the temperature dependence of ionic conductivity, SS|electrolyte|SS coin cells were prepared using SS disc electrodes (15.5 mm diameter); electrolytes were confined using an annular Teflon spacer (7.6 mm inner diameter and 1.6 mm thickness) placed between the SS electrodes. All coin cells were sealed using a digital pressure-controlled electric crimper (MTI Corp.).

Nuclear Magnetic Resonance Spectroscopy Measurements

A Bruker AVANCE III 500 MHz NMR spectrometer with a standard multinuclear broadband observe probe of the z-gradient was used to obtain 1D NMR spectra. Spectroscopy measurements were performed at room temperature (20 °C) and the nuclei examined were ^{7}Li and ^{19}F in order to observe the Li^+ and $TFSI^-$ local environments, respectively. The reference and locking solution used for all samples was 0.5 M LiTFSI in D_2O, and full NMR spectra with normalized reference peaks can be found in the Supporting Information (Figures S2 and S3), as well as tabulated peak positions and shifts (Tables S1 and S2). IL, SIL, and ZI monomer solutions were injected into glass capillary tubes (inner diameter 1.5 mm) that were placed into a standard NMR tube (inner diameter 5 mm) containing the reference solution. NMR chemical shift measurements were performed using a relaxation delay of 0.1 ms and a total of 32 scans.

The pulsed-field gradient spin-echo (PGSE) NMR method was employed to measure self-diffusivities of the Li^+ and $TFSI^-$ species. Samples were prepared in a N_2-filled glovebox by injecting IL, SIL, or ionogel precursor solutions containing a ZI monomer, IL/SIL, and photoinitiator in a standard NMR tube (inner diameter 5 mm). Ionogel samples were cured via UV irradiation for 10 minutes. NMR tubes were flame-sealed prior to performing the PGSE NMR measurements.

Proton diffusion coefficients were measured on a Bruker Avance III 400 MHz NMR spectrometer using a variable gradient bi-polar pulsed pair DOSY experiment with 500ms diffusion delays, 10ms gradient pulses, and a maximum gradient strength of 55 G/cm. Fluorine diffusion coefficients were measured similarly, but with 7.5ms gradient pulses instead. ^7Li diffusivities were measured on a Varian-Agilent Direct Digital Drive 300 MHz NMR with either spin-echo or stimulated pulse sequences appropriate to the relaxation times of the sample, delays ranging between 50-180ms, pulse widths of 1.5-4 ms, and a Doty Z-spec diffusion probe with maximum gradient strength of 1000 G/cm.

From the self-diffusivities determined by PGSE NMR, the lithium transport number (T_{Li^+}), or the fraction of total ionic species self-diffusion in the system due to Li^+, can be calculated.[47] As NMR will probe all species containing a particular element (regardless of coordination), correlating results from PGSE NMR to electrochemical performance requires understanding the degree of ion dissociation.[48,49] However, comparing changes in apparent self-diffusivities and T_{Li^+} values is a valuable method of probing ion mobility within the electrolyte environment. For the 1M LiTFSI/BMP TFSI electrolyte, there are three mobile ions in the system whose self-diffusivities can be measured (D_{Li^+}, D_{TFSI^-}, and D_{BMP^+}), so T_{Li^+} is calculated according to Equation (1):

$$T_{Li^+} = \frac{c_{Li^+}D_{Li^+}}{c_{Li^+}D_{Li^+} + c_{TFSI^-}D_{TFSI^-} + c_{BMP^+}D_{BMP^+}} \tag{1}$$

Where D_{Li^+}, D_{TFSI^-}, and D_{BMP^+} are the self-diffusivities determined by PGSE NMR spectroscopy and c_i are the respective molar concentrations for each ion. With only two mobile ions of equal concentrations, in SIL-based samples the calculation of T_{Li^+} values simplifies to Equation (2):

$$T_{Li^+} = \frac{D_{Li^+}}{D_{Li^+} + D_{TFSI^-}} \tag{2}$$

Electrochemical Measurements

All electrochemical measurements were performed using a VersaSTAT 3 potentiostat with a built-in frequency analyzer (Princeton Applied Research). AC impedance spectroscopy was used to measure ionic conductivities of the IL, SIL, and polyzwitterion-supported ionogels of both electrolyte systems. Room temperature ionic conductivity measurements were performed in a N_2-filled glovebox using a custom Teflon cell that was calibrated using three reference IL electrolyte samples of known ionic conductivities. Measurements were conducted over a frequency range of 1 Hz to 100 kHz using a sinusoidal voltage amplitude of 10 mV, and the ionic conductivity was calculated using the real impedance plateau value at high frequency, where the phase angle approached 0°. Temperature-dependent ionic conductivity measurements were performed using symmetric SS|electrolyte|SS coin cells secured to a temperature-controlled microscopy stage

(Linkam Scientific Instruments, LTS 420). A holding period of 10 minutes was utilized at each temperature during the heating and cooling cycles to ensure thermal equilibration, and all temperature-dependent Arrhenius model trend lines were fit with a R^2 value of 0.99 or higher. Linear sweep voltammetry (LSV) experiments were conducted with a scan rate of 1 mV s^{-1} using an asymmetric Li|electrolyte|SS cell with Li metal as the counter/reference electrode and stainless steel as the working electrode.

Symmetric Li|electrolyte|Li coin cells were prepared for determination of Li^+ transference numbers, and prior to DC polarization measurements, cells were preconditioned using a two-hour galvanostatic charge period at 0.01 mA cm^{-2}, followed by a two-hour potentiostatic hold, and finally a two-hour galvanostatic discharge at –0.01 mA cm^{-2}. After the preconditioning steps were completed, an additional 12 hour rest period was implemented before any experiments were performed. Determination of Li^+ transference numbers was conducted via DC polarization/chronoamperometry measurements using an applied potential of 10 mV for two hours, and AC impedance spectra were recorded both before and after the measurements. Using the method developed by Bruce and co-workers,[50,51] Li^+ transference number (t_{Li^+}) values were calculated according to Equation (3), employing the initial (I_0) and steady-state (I_{SS}) currents and the interfacial resistances measured via impedance spectroscopy before (R_0) and after (R_{SS}) DC polarization.

$$t_{Li^+} = \frac{I_{SS}(\Delta V - I_0 R_0)}{I_0(\Delta V - I_{SS} R_{SS})} \quad (3)$$

Equation (4) was used to calculate Li^+ conductivity (σ_{Li^+}) values using the room temperature total ionic conductivity (σ) of each electrolyte measured previously.

$$\sigma_{Li^+} = \sigma t_{Li^+} \quad (4)$$

RESULTS AND DISCUSSION

Prior to the investigation of ion transport in any ionogels, solutions of the four ZI monomers in each of the liquid electrolytes were used to probe the apparent interactions between the various ZI moieties and ions within these nonaqueous electrolytes. The upper limits of the ZI unit:Li^+ mole fraction values investigated were selected based on the criterion that each ZI monomer remain visually dissolved at room temperature at that concentration; in both of the liquid electrolytes employed here, SBVI was observed to be the least soluble monomer. 1D NMR chemical shifts of the ^7Li and ^{19}F nuclei were measured for each monomer solution at two different ZI unit:Li^+ mole fraction values. Analyzing the ^7Li and ^{19}F signal chemical shifts can provide insight into changes in the local environments of the Li^+ cations and $TFSI^-$ anions, respectively, in the presence of the ZI moieties. For these measurements, monomer solutions were used in order to avoid the significant peak broadening that can occur in polymerized ionogel samples. For 1M LiTFSI/BMP TFSI, monomer solutions containing ZI unit:Li^+ mole fraction values of 0.2 and 0.4 were prepared, and the resulting NMR spectra are compared to that of the neat solution in Figure 2.

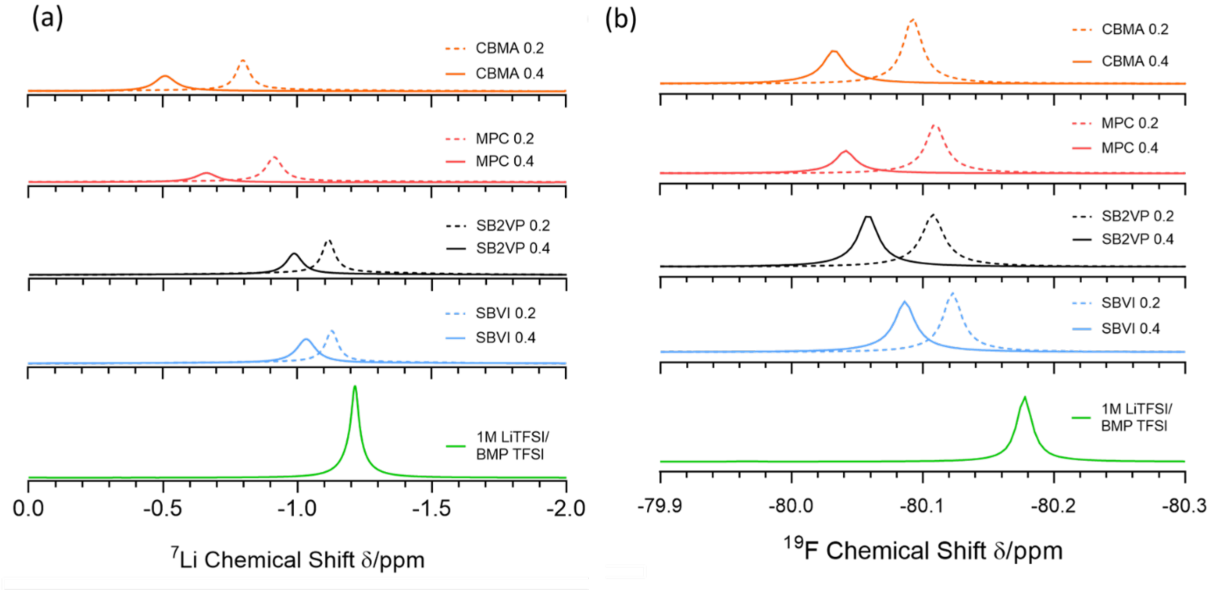

Figure 2. (a) ^{7}Li NMR spectra of 1M LiTFSI/BMP TFSI solution (bottom) and ZI monomer solutions containing CBMA, MPC, SB2VP, and SBVI at 0.2 and 0.4 ZI unit:Li^{+} mole fraction values. (b) ^{19}F NMR spectra of the same solutions.

As seen in Figure 2a, downfield shifts in the ^{7}Li NMR signal peak positions were observed for all ZI monomer solutions, relative to the peak position in the base IL solution electrolyte environment. This suggests that notable Coulombic interactions between each ZI monomer and Li^{+} cations occur to some degree, which likely disrupts the Li^{+}(TFSI^{-})$_{n}$ ion clusters originally present in the 1M LiTFSI/BMP TFSI electrolyte.[52,53] Notably, however, the magnitude of the chemical shift depends on the specific zwitterion chemistry (see Table S1 for a full summary of the peak shifts). The two sulfobetaine (SB) ZI monomers, SBVI and SB2VP, yield the smallest downfield ^{7}Li peak shifts ($\Delta\delta$ of 0.09 ppm and 0.11 ppm, respectively, for a ZI unit:Li^{+} mole fraction of 0.2). In comparison, at the same ZI unit:Li^{+} mole fraction of 0.2, the presence of MPC monomer results in a ^{7}Li peak shift of 0.31 ppm, while CBMA shifts the same peak by 0.43 ppm. Therefore, compared to the SB monomers, both the PC and CB zwitterions cause larger ^{7}Li chemical shifts in the 1M

LiTFSI/BMP TFSI solution, indicating a greater change in the Li^+ cation local environment. It was also noted that all peak shifts increased even further when the ZI unit:Li^+ mole fraction value was increased from 0.2 to 0.4.

A similar trend was observed for the ^{19}F chemical shifts in these solutions, as displayed in Figure 2b. At a ZI unit:Li^+ molar ratio of 0.4, the largest peak shift was observed for the CBMA solution, which moved from -80.18 ppm in the base IL electrolyte to -80.03 ppm. As with the ^7Li spectra, the ordering of ZI monomers for those causing the largest to smallest peak shifts was: CBMA > MPC > SB2VP > SBVI. The fact that SBVI solutions yielded the smallest chemical shift changes is consistent with our observation that this monomer displayed the lowest solubility in the base liquid electrolyte. A previous study in our group revealed that MPC was more interactive with Li^+ ions in the 1M LiTFSI/BMP TFSI environment compared to SBVI,[39] and these results are consistent with our previous observations. The SB2VP solution spectra obtained in this work reveal a consistent theme of relatively low SB zwitterion-ion interactions in this particular IL-based electrolyte. Importantly, as shown by Figure 2a, CBMA actually produced an even larger Li^+ peak shift than MPC. Strong interactions between CBMA and cations such as Li^+ have been previously revealed in aqueous environments, attributable to a larger difference in cationic and anionic group charge densities (*e.g.* compared to SB zwitterions),[42,43] and the present results confirm that similar observations can be true for an IL environment, as well.

The four ZI monomers were also studied in a lithium-containing SIL electrolyte, [Li(G4)][TFSI]. As noted previously, SILs have been shown to demonstrate similar properties to conventional ionic liquids. However, the nature of interaction between a ZI moiety and the glyme-wrapped Li^+ complex cation is not yet well understood.[40] In addition to its G4-complexed Li^+ cation, it is also important to note that the concentration of Li^+ in [Li(G4)][TFSI] is approximately 2.8M, which is nearly three times higher than in the 1M LiTFSI/BMP TFSI electrolyte. Therefore, ZI unit:Li$^+$ mole fraction values of 0.1 and 0.2 were studied in the SIL system, which correspond to nearly equivalent total ZI unit concentrations (on a mol/L basis) as those examined in the conventional IL solution electrolyte, approximately 0.3M to 0.7M.

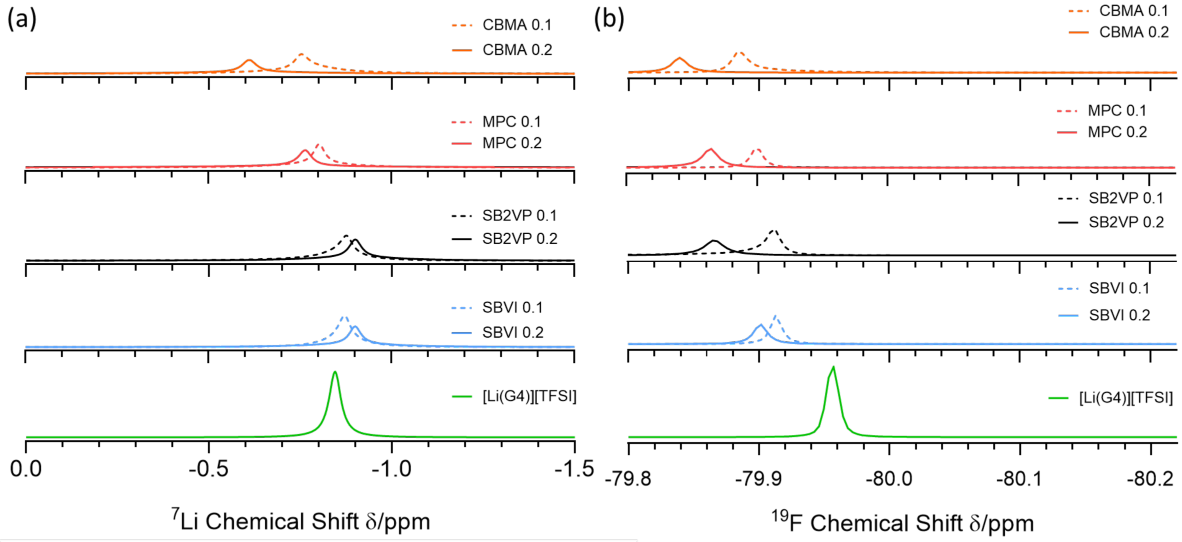

Figure 3. (a) ^{7}Li NMR spectra of SIL electrolyte, [Li(G4)][TFSI], (bottom) and ZI monomer solutions containing CBMA, MPC, SB2VP, and SBVI at 0.1 and 0.2 ZI unit:Li$^+$ mole fraction values. (b) ^{19}F NMR spectra of the same solutions.

Figure 3 displays the ^{7}Li and ^{19}F NMR spectra of the ZI monomer solutions prepared in [Li(G4)][TFSI] with ZI unit:Li$^+$ molar fractions of 0.1 and 0.2, along with the neat SIL. Compared with the peak shifts observed in the 1M LiTFSI/BMP TFSI electrolyte (Fig. 2), several differences could be observed for the ZI monomer/SIL solutions. While the MPC and CBMA monomer solutions displayed downfield peak shifts as in the conventional IL solution, both of the SB monomers (SBVI and SB2VP) generated modest upfield ^{7}Li peak shifts. This is consistent with our observation of even lower solubility of the SB monomers in SIL compared to that in the conventional IL solution, and is likely due to subtle changes in the $TFSI^-$/SB monomer/$[Li(G4)]^+$ local coordination structure(s) that result in greater shielding of the Li nucleus. In addition, for the same ZI unit:Li^+ molar fraction value of 0.2 in each electrolyte, the magnitudes of both the ^7Li and ^{19}F peak shifts were smaller for all ZI monomer solutions in the SIL (see Table S2). These observations support the hypothesis that the strong coordination of Li^+ by G4 largely persists in the presence of these ZI monomers (especially SBVI and SB2VP), which hinders zwitterion-Li^+ interactions. It was noted, however, that CBMA produced the greatest downfield shift in the ^7Li peak position, and that its difference in peak shift was the largest when the ZI unit:Li^+ molar fraction value doubled from 0.1 to 0.2. This suggests that, just as in the 1M LiTFSI/BMP TFSI electrolyte, CBMA-Li^+ interactions are the most significant among this diverse group of ZI monomers. Finally, it is common to observe some peak broadening upon the addition of ZI monomers to the IL electrolytes, due to an increase in solution viscosity. However, all of our Li^+ transport measurements (*vide infra*) were performed on ZI homopolymer-supported ionogels, not monomer solutions, as the formation of a 3D polymeric scaffold that spans the ionogel presents new potential pathways for ion conduction that do not exist in a monomer solution.

ZI monomers were polymerized *in situ* via UV-initiated free radical polymerization within the two lithium-containing IL types to create homopolymer support scaffolds (*e.g.* pCBMA, poly(carboxybetaine methacrylate)) for the resulting ionogel electrolytes. Photopolymerization in ILs has been well studied, and it has been established that ILs increase polymerization rates and radical lifetimes, which leads to higher molecular weights and high overall monomer conversion.[54–56] Here, as in our previous studies, gels are formed by *in situ* polymerization in small IL volumes, and therefore it is assumed that all monomer conversions approached 100%. All gels synthesized in 1M LiTFSI/BMP TFSI were made using a ZI unit:Li^+ mole fraction value of 0.3

(this corresponds to an approximate polymer content of 5 wt% for the pCBMA, pSB2VP, and pSBVI samples, and 6 wt% for pMPC gels), while all gels synthesized in [Li(G4)][TFSI] contained a ZI unit:Li^+ mole fraction value of 0.15 (approximately 8 wt% polymer for the pCBMA, pSB2VP, and pSBVI samples, and 11 wt% for pMPC gels). Photographs of representative polyzwitterion-supported gels prepared in standard NMR tubes, compared with both liquid electrolytes, are shown in Figure 4. Notably, while all eight of the monomer solutions at these concentrations formed transparent, homogeneous solutions, most of the gels were somewhat opaque in appearance, with the exception of the pMPC-supported ionogels (Fig. 4). This indicates that the remaining three polyzwitterion scaffolds (pCBMA, pSB2VP, and pSBVI) were not fully miscible with these IL electrolytes, likely due to significant ZI group self-association. It is noted that pMPC, whose monomer possesses the highest molar mass among the four ZI units studied here and therefore yields the highest homopolymer weight fraction in each gel type, still shows the best compatibility in both liquids. Interestingly, the two SB-type homopolymer-supported gels displayed visible pink to orange/yellow colorations in the SIL (Fig. 4b). We posit that these colors may be due to extended pi-pi stacking aggregates that form among the pyridinium or imidazolium units present on the SB2VP and SBVI units, respectively; however, further structural characterization is ongoing and outside the scope of this study. The differences in miscibility between the various polyzwitterions examined here may also be expected to have an influence on ion transport within these gel electrolytes, as discussed below.

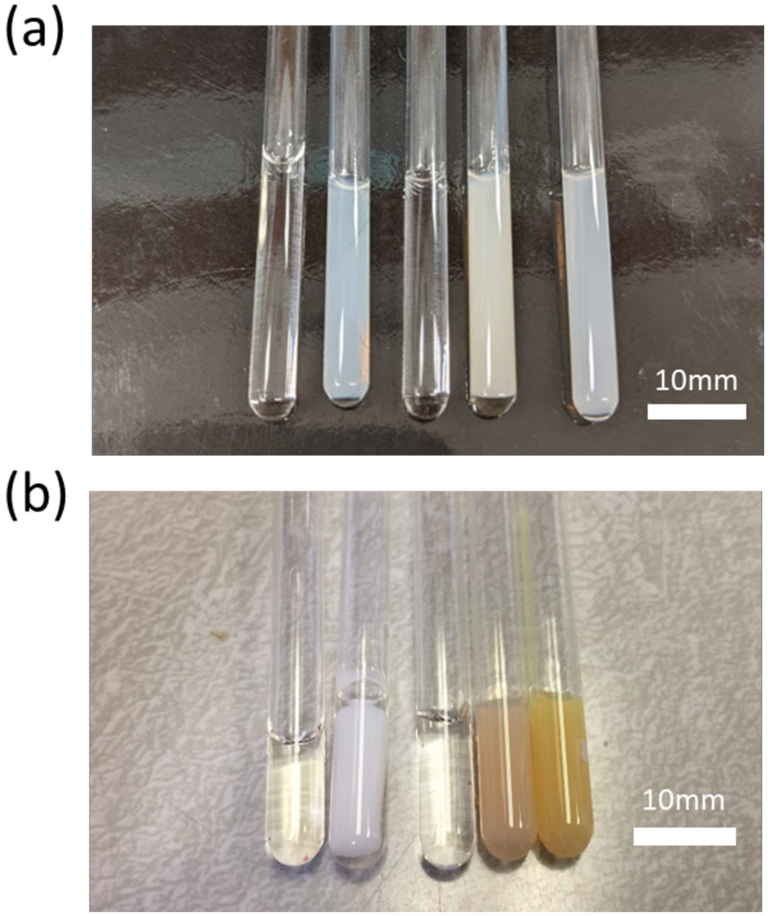

Figure 4. Photographs of electrolyte samples in standard NMR tubes. (a) 1M LiTFSI/BMP TFSI liquid electrolyte and ZI homopolymer-supported ionogels formed *in situ* within this liquid, using a ZI unit:Li$^+$ mole fraction value of 0.3. From left to right: IL solution electrolyte, pCBMA-, pMPC-, pSB2VP-, and pSBVI-supported gels. (b) [Li(G4)][TFSI] SIL and ZI homopolymer-supported ionogels formed *in situ* within this liquid, using a ZI unit:Li$^+$ mole fraction value of 0.15. From left to right: SIL electrolyte, pCBMA-, pMPC-, pSB2VP-, and pSBVI-supported gels.

Pulsed-field gradient spin echo (PGSE) NMR spectroscopy was utilized to measure apparent ion self-diffusivities in the two liquid electrolytes and their polyzwitterion-supported gel samples. For the 1M LiTFSI/BMP TFSI electrolyte, self-diffusivities of the Li^+ and BMP^+ cations and the $TFSI^-$ anion were measured and the values reported in Table 1. For this electrolyte, D_{proton} values refer to self-diffusivity of the BMP^+ cation, which is the only mobile proton-bearing species in the liquid. As seen in Table 1, there was a clear *increase* in all ionic species self-diffusivities across all four of the polyzwitterion-supported gels, as compared to the base IL electrolyte. The increased self-diffusivities of all ions suggest that these four ZI homopolymers all promote enhanced ion cluster/pair dissociation in this electrolyte through Coulombic interactions, which in turn boosts the apparent (average) ion mobilities. Lithium-ion *transport* number values (T_{Li}^+), based on ion self-diffusivity values, were calculated as described by Equation (1) (see Experimental Methods). Without knowing the degree of ion pair/cluster dissociation within the system, it is difficult to make direct correlations between PGSE NMR diffusivities and ionic conductivity.[48,49] However, calculation of T_{Li}^+ values here still provides insight into how the presence of each polyzwitterion impacts the electrolyte, and, as shown in Table 1, all of the ZI scaffolds yielded modest increases in gel T_{Li}^+ values compared with that of the 1M LiTFSI/BMP TFSI solution. The largest T_{Li}^+ value increase (0.098 vs. 0.070) was seen in the case of the pSB2VP gel, which also displayed the largest increase in Li^+ cation self-diffusivity (5.7×10^{-12} m^2 s^{-1} vs. 2.1×10^{-12} m^2 s^{-1}).

A different overall trend was observed for the [Li(G4)][TFSI] SIL electrolyte system, however, wherein three out of the four polyzwitterion scaffolds led to a clear *decrease* across all species self-diffusivity values (for the pMPC, pSBVI, and pSB2VP gels). This may possibly be due to stronger Coulombic ZI unit-ion interactions in this electrolyte, for which no second cation is present (*i.e.* no BMP^+), resulting mostly in ion "trapping" by the ZI units rather than ion pair/cluster dissociation. It should be noted that for the SIL-based samples, D_{proton} in Table 1 refers to the self-diffusivity of tetraglyme (G4), which should, in principle, agree well with the D_{Li^+} value in each case if the $[Li(G4)]^+$ complex cations remain intact.[57,58] Upon calculating T_{Li^+} values for the SIL-based samples, it can be seen that for the pMPC gel in particular, a notable increase in T_{Li^+} was observed (0.55 vs. 0.48 in the SIL), which corresponded to the largest decrease in $TFSI^-$ anion self-diffusivity ($4.1 \times 10^{-12}\ m^2\ s^{-1}$ vs. $8.3 \times 10^{-12}\ m^2\ s^{-1}$ in the SIL). On this point, it is noteworthy that pMPC is the only ZI homopolymer examined here for which the cationic (ammonium) portion of the ZI unit is oriented outward, located furthest away from the polymerizable group (see Fig. 1). Strikingly, the pCBMA gel prepared in SIL displayed notable *increases* in all species self-diffusivities compared to the liquid electrolyte. In this regard, the pCBMA scaffold in SIL appears to act more similarly to how it does in 1M LiTFSI/BMP TFSI than the other three ZI homopolymers. In addition, it can be seen that the difference between the apparent Li^+ and G4 self-diffusivity values is greatest in the pCBMA gel, for which D_{Li^+} and D_{proton} were measured to be $12.5 \times 10^{-12}\ m^2\ s^{-1}$ and $15.7 \times 10^{-12}\ m^2\ s^{-1}$, respectively. This indicates that there is some degree of breakup of the $[Li(G4)]^+$ complexes, and that a fraction of each species can diffuse independently of the other. Here, it should be recalled that the ^7Li NMR chemical shifts were also found to be the most dramatic for the pCBMA gels among the SIL-based samples (see Fig. 3a).

Table 1. Self-diffusivity values measured by PGSE NMR spectroscopy of Li^+, $TFSI^-$, and either BMP^+ ions (in the 1M LiTFSI/BMP TFSI-based samples) or tetraglyme molecules (in the Li(G4)][TFSI]-based samples), denoted as D_{proton}. Lithium-ion transport number ($T_{Li}{}^+$) values calculated from these self-diffusivities.

Sample	D_{Li+} [10^{-12} m^2 s^{-1}]	D_{TFSI-} [10^{-12} m^2 s^{-1}]	D_{proton} [10^{-12} m^2 s^{-1}]	T_{Li+}
1M LiTFSI/BMP TFSI	2.1	2.9	5.0	0.070
pCBMA 0.3	4.2	6.0	8.2	0.076
pMPC 0.3	4.1	5.6	7.7	0.079
pSB2VP 0.3	5.7	6.6	7.8	0.098
pSBVI 0.3	4.3	5.7	6.3	0.090
[Li(G4)][TFSI]	7.7	8.3	7.9	0.48
pCBMA 0.15	12.5	12.1	15.7	0.51
pMPC 0.15	5.1	4.1	5.2	0.55
pSB2VP 0.15	5.4	5.7	5.9	0.49
pSBVI 0.15	6.7	7.8	7.6	0.46

The temperature dependence of total ionic conductivity near ambient conditions (approximately 0 °C to 80 °C) and room temperature lithium-ion *transference* number values (t_{Li^+}, the fraction of total current carried by Li^+ in an applied electric field) were measured for the same electrolyte formulations using AC impedance spectroscopy and DC polarization, respectively. Table 2 summarizes key metrics of the 1M LiTFSI/BMP TFSI and [Li(G4)][TFSI] SIL electrolytes, as well as of their corresponding polyzwitterion-supported ionogels. Temperature-dependent ionic conductivity data for all samples, as well as DC polarization and AC impedance spectroscopy data used to determine t_{Li^+} values, can be found in the Supporting Information (Figures S4-S7 and Tables S3-S4). In the 1M LiTFSI/BMP TFSI electrolyte, all four of the polyzwitterion gels exhibited room temperature ionic conductivity (σ) values that were approximately equal to or slightly larger than the IL solution, despite having, by definition, a lower ion concentration in the gel samples. This is consistent with the increased ion self-diffusivities observed for these gels (Table 1), as well as our hypothesis that the ZI groups promote a higher degree of ion cluster/pair dissociation in this electrolyte. Moreover, for the two gels that exhibited the largest room temperature ionic conductivities (pCMBA and pMPC gels), we also observed the lowest apparent activation energy of ionic conductivity (E_a) values obtained from Arrhenius model fits, which were both lower than that of the 1M LiTFSI/BMP TFSI solution itself. This indicates a clear improvement in the ease of overall ion transport within gels containing these two specific zwitterion chemistries, and it is also consistent with our previous study of a pMPC-rich copolymer-supported gel in the same IL solution.[39]

Lithium-ion transference number values (t_{Li^+}) showed a similar trend for the 1M LiTFSI/BMP TFSI-based samples, with the largest enhancement seen for the pCBMA and pMPC gels (0.37 and 0.38, respectively, versus 0.23 for the IL solution). Maximizing t_{Li^+} is desirable for Li-ion battery electrolytes because it helps to minimize undesirable side reactions from occurring due to concentration polarization of BMP^+ and $TFSI^-$ ions at the electrode interfaces.[59–61] In addition, a higher t_{Li^+} contributes to improved room temperature lithium-ion conductivity values (σ_{Li^+}), which were as high as 0.37 mS cm^{-1} for the pCBMA gel. Notably, the two polyzwitterions that provided the largest boost in Li^+ transport (pCBMA and pMPC gels) also exhibited the largest downfield chemical shifts in the ^{7}Li NMR spectra of their monomer solutions (Fig. 2a), which suggests a possible correlation between these measurements. It is also worth noting that there were differences in ionogel/Li interfacial resistances observed between the four polyzwitterions; the pSBVP scaffold in particular led to much higher interfacial resistance in both electrolyte types (Figs. S5 and S7), suggesting lower compatibility with lithium metal.

Within the SIL electrolyte environment, a remarkable difference in behavior was observed when comparing the pCBMA sample to the other three polyzwitterion chemistries. As shown in Table 2, most of the polyzwitterion-supported gels (except for pCMBA) showed a clear decrease in room temperature ionic conductivity values compared to that of the neat SIL. This is consistent with the lower ion self-diffusivity values measured within these formulations (see Table 1), as well as our previous study of a pMPC-co-pSBVI gel scaffold in [Li(G4)][TFSI].[40] On the other hand, the pCBMA scaffold in SIL behavior is unique (among the polyzwitterions examined in this study): it appears to promote greater ion pair/cluster dissociation and thus exhibits a ZI gel ionic conductivity that is essentially equal to that of SIL itself (despite having a lower ion concentration). This is further supported by the observed difference between the apparent self-diffusivities of the Li^+ and G4 species in the pCBMA-supported SIL gel that suggest that pCBMA disrupts the cation complex, yielding some fraction of uncomplexed Li^+ ions, similar to the conventional IL solution. One key difference, however, is that the pCBMA gel E_a value was not significantly lower than that of the neat SIL (to within error); this may be the result of lower solubility of pCBMA in the SIL vs. 1M LiTFSI/BMP TFSI (see Fig. 4), which led to larger polymer aggregate sizes and reduced the effective number of ZI unit-ion interactions. While the pCBMA gels showed visible evidence of polymer aggregation, this does not preclude the ability of a significant number of CB groups to still interact with Li^+ at the scaffold/liquid interface. It is possible that the pCBMA scaffold, while not highly dispersed, nevertheless promotes a much higher fraction of dissociated / "free" Li^+ ions that results in the observed improved Li^+ transport. Future experimental and molecular dynamics (MD) simulation studies are needed to probe these effects and to decouple polymer solubility differences from ionogel ion transport measurements. Nevertheless, it should be noted that the pCBMA-supported SIL gel displayed the highest σ_{Li^+} value of all electrolytes examined here, at 0.44 mS cm^{-1}. This value exceeds our previous record for a polyzwitterion-supported SIL gel (σ_{Li^+} of 0.29 mS cm^{-1} for 20 mol% pMPC in [Li(G4)][TFSI]).[40] Finally, this enhancement of Li^+ transport in the pCBMA gel is also seen to correlate with the CBMA monomer solution yielding the largest downfield chemical shift in the ^7Li NMR spectral peak compared with the SIL (Fig. 3a), which further supports our hypothesis that the behavior of this particular polyzwitterion gel is more comparable to its 1M LiTFSI/BMP TFSI analogue. It may also suggest that seeing a significant downfield shift in the ^7Li NMR peak position of other, heretofore unexplored ZI monomers could possibly be a predictor of improved Li^+ transport in their corresponding polyzwitterion-supported ionogel electrolytes. If shown to be generally true, this could prove to be a useful way to screen a large number of ZI moieties for their potential to increase lithium-ion conductivity within future ionic liquid-based/polyzwitterion composite electrolytes.

Table 2. Summary of room temperature ionic conductivity (σ), activation energy of total ionic conductivity (E_a), lithium-ion transference number (t_{Li^+}) and room temperature Li^+ conductivity (σ_{Li^+}) values for the 1M LiTFSI/BMP TFSI and [Li(G4)][TFSI] SIL electrolytes and their corresponding polyzwitterion-supported gels.

Sample	**σ [mS cm^{-1}] ±0.10 mS cm^{-1}**	**E_a [kJ mol^{-1}] ±1.0 kJ mol^{-1}**	t_{Li^+}	σ_{Li^+} **[mS cm^{-1}]**
1M LiTFSI/BMP TFSI	0.90	29.2	0.23	0.21
pCBMA 0.3	1.00	24.6	0.37	0.37
pMPC 0.3	0.96	25.4	0.38	0.36
pSB2VP 0.3	0.91	29.1	0.28	0.26
pSBVI 0.3	0.94	28.2	0.31	0.29
[Li(G4)][TFSI]	1.20	27.1	0.19	0.23
pCBMA 0.15	1.20	26.6	0.37	0.44
pMPC 0.15	0.82	29.5	0.41	0.34
pSB2VP 0.15	0.90	28.7	0.40	0.36
pSBVI 0.15	0.91	26.5	0.23	0.21

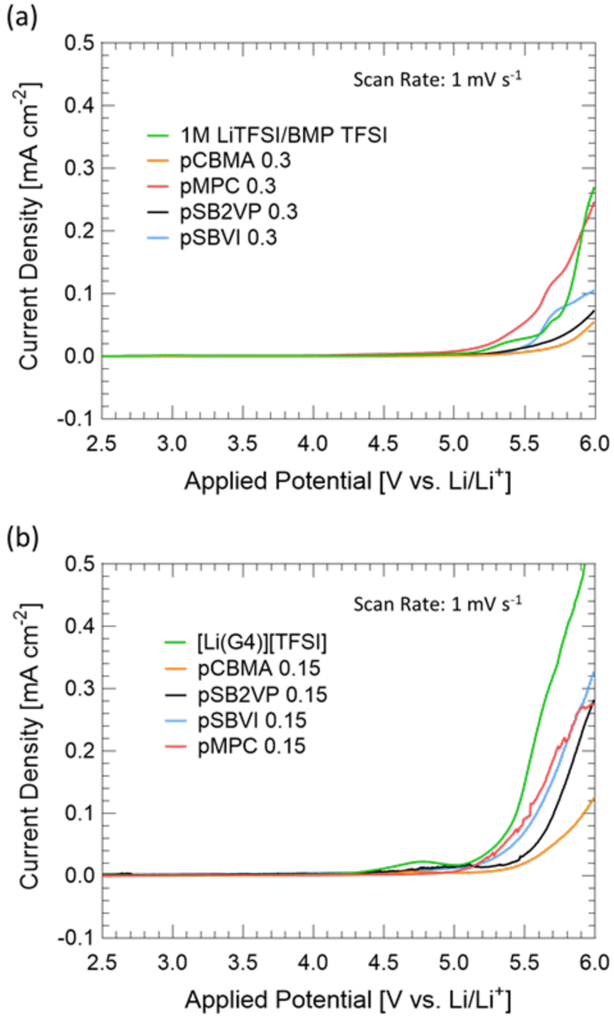

Figure 5. Linear sweep voltammograms for the neat liquid electrolytes and their polyzwitterion-supported gels. (a) 1M LiTFSI/BMP TFSI-based electrolytes. (b) [Li(G4)][TFSI] SIL-based electrolytes. Measurements performed using a scan rate of 1 mV s^{-1} with a stainless steel working electrode.

Anodic electrochemical stability of the ionic liquid and polyzwitterion gel electrolytes was examined using linear sweep voltammetry (LSV). As seen in Figure 5a for the 1 M LiTFSI/BMP TFSI-based electrolytes, all formulations displayed high stability exceeding 5.0 V versus Li/Li^+. The majority of the polyzwitterion-supported gels also showed a slight increase in anodic stability compared to the IL solution, with the exception of pMPC. While not the focus of this study, additional electrochemical characterization to understand these subtle differences in ionogel anodic stability observed between the various polyzwitterion chemistries could be of interest for a future investigation. Figure 5b shows the LSV curves obtained for the SIL-based electrolytes, which also illustrates that the presence of the polyzwitterions may provide a slight benefit to the anodic stability of the electrolyte. When comparing the two electrolyte systems, it is worth noting that the onset of instability occurs at slightly lower voltages for the [Li(G4)][TFSI] system compared to the 1M LiTFSI/BMP TFSI, which may be due to the glyme having lower stability than the ILs.[62] Notably, in can be seen that in both ionic liquid electrolyte types, pCBMA stands out as promoting the highest anodic stability among the four polyzwitterions, which further supports the idea that CB-type zwitterions may hold substantial promise for the future design of ionogel electrolytes for lithium-based batteries, as the pCBMA gels were also found to exhibit the largest σ_{Li^+} values in this study.

CONCLUSIONS

The spectroscopic, ion transport properties, and electrochemical stability of ionogel electrolytes containing four distinct ZI homopolymers were examined in both a conventional lithium-containing IL solution and a SIL. It was found that the impact of polyzwitterions on Li^+ transport in these two ionic liquid electrolyte classes depends both on zwitterion chemistry and the specific electrolyte environment. In the 1M LiTFSI/BMP TFSI system, strong Coulombic interactions between ZI units and ions led to increased ion pair/cluster dissociation and boosted overall ion transport. In the SIL electrolyte, the presence of the SB and PC polyzwitterions tended to slow down ion motion, while the CB-type polyzwitterion (pCBMA) exhibited behavior that was more characteristic of that in the conventional IL/lithium salt environment. In both electrolytes, the addition of pCBMA resulted in a significant boost in selective Li^+ transport, and it is noteworthy that this monomer also caused the largest downfield ^7Li NMR peak shift in both electrolytes, which suggests that ^7Li NMR may potentially be a quick and effective screening tool for predicting the lithium-ion transport facility of novel ZI polymer-supported ionogel electrolytes. Based on these results, future work will aim to incorporate electrolytes containing pCBMA into lithium-based batteries and study the impact of ZI polymer scaffolds on overall battery performance and long-term stability.

ACKNOWLEDGEMENTS

This work was performed with support from the National Science Foundation (CBET-1802729) and from Tufts University. The NMR measurements conducted at Hunter College were supported by grant no. N00014-20-1-2186 from the U.S. Office of Naval Research.

SUPPORTING INFORMATION

CBMA monomer ^1H NMR spectrum, additional NMR spectra with tabulated peak positions, temperature-dependent ionic conductivity data, and a summary of the lithium-ion transference number measurements, including Nyquist plots recorded before/after polarization (PDF)

REFERENCES

(1) Bruce, P. G. Energy Storage beyond the Horizon: Rechargeable Lithium Batteries. *Solid State Ionics* **2008**, *179*, 752–760.

(2) Morris, M. A.; An, H.; Lutkenhaus, J. L.; Epps, T. H. Harnessing the Power of Plastics: Nanostructured Polymer Systems in Lithium-Ion Batteries. *ACS Energy Lett.* **2017**, *2*, 1919–1936.

(3) Marom, R.; Amalraj, S. F.; Leifer, N.; Jacob, D.; Aurbach, D. A Review of Advanced and Practical Lithium Battery Materials. *J. Mater. Chem.* **2011**, *21*, 9938–9954.

(4) Chen, J. Recent Progress in Advanced Materials for Lithium Ion Batteries. *Materials* **2013**, *6*, 156–183.

(5) Armand, M.; Endres, F.; MacFarlane, D. R.; Ohno, H.; Scrosati, B. Ionic-Liquid Materials for the Electrochemical Challenges of the Future. *Nat. Mater.* **2009**, *8*, 621–629.

(6) Galiński, M.; Lewandowski, A.; Stepniak, I. Ionic Liquids as Electrolytes. *Electrochim. Acta* **2006**, *51*, 5567–5580.

(7) MacFarlane, D. R.; Tachikawa, N.; Forsyth, M.; Pringle, J. M.; Howlett, P. C.; Elliott, G. D.; Davis, J. H.; Watanabe, M.; Simon, P.; Angell, C. a. Energy Applications of Ionic Liquids. *Energy Environ. Sci.* **2014**, *7*, 232–250.

(8) Marr, P. C.; Marr, A. C. Ionic Liquid Gel Materials: Applications in Green and Sustainable Chemistry. *Green Chem.* **2015**, *18*, 105–128.

(9) Pappenfus, T. M.; Henderson, W. A.; Owens, B. B.; Mann, K. R.; Smyrl, W. H. Complexes of Lithium Imide Salts with Tetraglyme and Their Polyelectrolyte Composite Materials. *J. Electrochem. Soc.* **2004**, *151*, A209-A215.

(10) Terada, S.; Ikeda, K.; Ueno, K.; Dokko, K.; Watanabe, M. Liquid Structures and Transport Properties of Lithium Bis(Fluorosulfonyl)Amide/Glyme Solvate Ionic Liquids

for Lithium Batteries. *Aust. J. Chem.* **2019**, *72*, 70–80.

(11) Ueno, K.; Yoshida, K.; Tsuchiya, M.; Tachikawa, N.; Dokko, K.; Watanabe, M. Glyme-Lithium Salt Equimolar Molten Mixtures: Concentrated Solutions or Solvate Ionic Liquids? *J. Phys. Chem. B* **2012**, *116*, 11323–11331.

(12) Kitazawa, Y.; Iwata, K.; Imaizumi, S.; Ahn, H.; Kim, S. Y.; Ueno, K.; Park, M. J.; Watanabe, M. Gelation of Solvate Ionic Liquid by Self-Assembly of Block Copolymer and Characterization as Polymer Electrolyte. *Macromolecules* **2014**, *47*, 6009–6016.

(13) Chen, Z.; Fitzgerald, P. A.; Warr, G. G.; Atkin, R. Conformation of Poly(Ethylene Oxide) Dissolved in the Solvate Ionic Liquid [Li(G4)]TFSI. *Phys. Chem. Chem. Phys.* **2015**, *17*, 14872–14878.

(14) Mandai, T.; Yoshida, K.; Ueno, K.; Dokko, K.; Watanabe, M. Criteria for Solvate Ionic Liquids. *Phys. Chem. Chem. Phys.* **2014**, *16*, 8761–8772.

(15) Shaplov, A. S.; Marcilla, R.; Mecerreyes, D. Recent Advances in Innovative Polymer Electrolytes based on Poly(ionic liquid)s. *Electrochim. Acta* **2015**, *175*, 18–34.

(16) Visentin, A. F.; Alimena, S.; Panzer, M. J. Influence of Ionic Liquid Selection on the Properties of Poly(Ethylene Glycol) Diacrylate-Supported Ionogels as Solid Electrolytes. *ChemElectroChem* **2014**, *1*, 718–721.

(17) Lin, D.; Liu, W.; Liu, Y.; Lee, H. R.; Hsu, P.-C.; Liu, K.; Cui, Y. High Ionic Conductivity of Composite Solid Polymer Electrolyte via In Situ Synthesis of Monodispersed SiO_2 Nanospheres in Poly(Ethylene Oxide). *Nano Lett.* **2016**, *16*, 459–465.

(18) Osada, I.; De Vries, H.; Scrosati, B.; Passerini, S. Ionic-Liquid-Based Polymer

Electrolytes for Battery Applications. *Angew. Chem. Int. Ed.* **2016**, *55*, 500–513.

(19) Ueno, K. Soft Materials Based on Colloidal Self-Assembly in Ionic Liquids. *Polym. J.* **2018**, *50*, 951–958.

(20) Le Bideau, J.; Viau, L.; Vioux, A. Ionogels, Ionic Liquid Based Hybrid Materials. *Chem. Soc. Rev.* **2011**, *40*, 907–925.

(21) Visentin, A. F.; Panzer, M. J. Poly(Ethylene Glycol) Diacrylate-Supported Ionogels with Consistent Capacitive Behavior and Tunable Elastic Response. *ACS Appl. Mater. Interfaces* **2012**, *4*, 2836–2839.

(22) Bin, A.; Susan, H.; Kaneko, T.; Noda, A.; Watanabe, M.; Susan, M. A. B. H.; Kaneko, T.; Noda, A.; Watanabe, M. Ion Gels Prepared by in Situ Radical Polymerization of Vinyl Monomers in an Ionic Liquid and Their Characterization as Polymer Electrolytes. *J. Am. Chem. Soc.* **2005**, *127*, 4976–4983.

(23) Shin, J. H.; Henderson, W. A.; Passerini, S. Ionic Liquids to the Rescue? Overcoming the Ionic Conductivity Limitations of Polymer Electrolytes. *Electrochem. Commun.* **2003**, *5*, 1016–1020.

(24) Meabe, L.; Huynh, T. V.; Mantione, D.; Porcarelli, L.; Li, C.; O’Dell, L. A.; Sardon, H.; Armand, M.; Forsyth, M.; Mecerreyes, D. UV-Cross-Linked Poly(Ethylene Oxide Carbonate) as Free Standing Solid Polymer Electrolyte for Lithium Batteries. *Electrochim. Acta* **2019**, *302*, 414–421.

(25) Shalu, S.; Singh, V. K.; Singh, R. K. Development of Ion Conducting Polymer Gel Electrolyte Membranes Based on Polymer PVdF-HFP, BMIMTFSI Ionic Liquid and the

Li-Salt with Improved Electrical, Thermal and Structural Properties. *J. Mater. Chem. C* **2015**, *3*, 7305–7318.

(26) Yeon, S. H.; Kim, K. S.; Choi, S.; Cha, J. H.; Lee, H. Characterization of PVdF(HFP) Gel Electrolytes Based on 1-(2-Hydroxyethyl)-3-Methyl Imidazolium Ionic Liquids. *J. Phys. Chem. B* **2005**, *109*, 17928–17935.

(27) Li, B.; Jain, P.; Ma, J.; Smith, J. K.; Yuan, Z.; Hung, H. C.; He, Y.; Lin, X.; Wu, K.; Pfaendtner, J.; Jiang, S. Trimethylamine N-Oxide–Derived Zwitterionic Polymers: A New Class of Ultralow Fouling Bioinspired Materials. *Sci. Adv.* **2019**, *5*, eaaw9562.

(28) Bengani-Lutz, P.; Converse, E.; Cebe, P.; Asatekin, A. Self-Assembling Zwitterionic Copolymers as Membrane Selective Layers with Excellent Fouling Resistance: Effect of Zwitterion Chemistry. *ACS Appl. Mater. Interfaces* **2017**, *9*, 20859–20872.

(29) Blackman, L. D.; Gunatillake, P. A.; Cass, P.; Locock, K. E. S. An Introduction to Zwitterionic Polymer Behavior and Applications in Solution and at Surfaces. *Chem. Soc. Rev.* **2019**, *48*, 757–770.

(30) Xuan, F.; Liu, J. Preparation, Characterization and Application of Zwitterionic Polymers Andmembranes: Current Developments and Perspective. *Polym. Int.* **2009**, *58*, 1350–1361.

(31) Vasantha, V. A.; Jana, S.; Parthiban, A.; Vancso, J. G. Water Swelling, Brine Soluble Imidazole Based Zwitterionic Polymers – Synthesis and Study of Reversible UCST Behaviour and Gel–Sol Transitions. *Chem. Commun.* **2014**, *50*, 46–48.

(32) Ning, J.; Li, G.; Haraguchi, K. Synthesis of Highly Stretchable, Mechanically Tough,

Zwitterionic Sulfobetaine Nanocomposite Gels with Controlled Thermosensitivities. *Macromolecules* **2013**, *46*, 5317–5328.

(33) Byrne, N.; Howlett, P. C.; MacFarlane, D. R.; Forsyth, M. The Zwitterion Effect in Ionic Liquids: Towards Practical Rechargeable Lithium-Metal Batteries. *Adv. Mater.* **2005**, *17*, 2497–2501.

(34) Yoshizawa, M.; Hirao, M.; Ito-Akita, K.; Ohno, H. Ion Conduction in Zwitterionic-Type Molten Salts and Their Polymers. *J. Mater. Chem.* **2001**, *11*, 1057–1062.

(35) Narita, A.; Shibayama, W.; Ohno, H. Structural Factors to Improve Physico-Chemical Properties of Zwitterions as Ion Conductive Matrices. *J. Mater. Chem.* **2006**, *16*, 1475-1482.

(36) Marwanta, E.; Mizumo, T.; Ohno, H. Improved Ionic Conductivity of Nitrile Rubber/Li(CF3SO2)2N Composites by Adding Imidazolium-Type Zwitterion. *Solid State Ionics* **2007**, *178*, 227–232.

(37) Lind, F.; Rebollar, L.; Bengani-Lutz, P.; Asatekin, A.; Panzer, M. J. Zwitterion-Containing Ionogel Electrolytes. *Chem. Mater.* **2016**, *28*, 8480–8483.

(38) Taylor, M. E.; Panzer, M. J. Fully-Zwitterionic Polymer-Supported Ionogel Electrolytes Featuring a Hydrophobic Ionic Liquid. *J. Phys. Chem. B* **2018**, *122*, 8469–8476.

(39) D'Angelo, A. J.; Panzer, M. J. Decoupling the Ionic Conductivity and Elastic Modulus of Gel Electrolytes : Fully Zwitterionic Copolymer Scaffolds in Lithium Salt / Ionic Liquid Solutions. *Adv. Energy Mater.* **2018**, *8*, *1801646*.

(40) D’Angelo, A. J.; Panzer, M. J. Design of Stretchable and Self-Healing Gel Electrolytes via

Fully Zwitterionic Polymer Networks in Solvate Ionic Liquids for Li-Based Batteries. *Chem. Mater.* **2019**, *31,* 2913-2922.

(41) Qin, H.; Panzer, M. J. Zwitterionic Copolymer-Supported Ionogel Electrolytes Featuring a Sodium Salt/Ionic Liquid Solution. *Chem. Mater.* **2020**, *32*, 7951–7957.

(42) Shao, Q.; He, Y.; Jiang, S. Molecular Dynamics Simulation Study of Ion Interactions with Zwitterions. *J. Phys. Chem. B* **2011**, *115*, 8358–8363.

(43) Shao, Q.; Mi, L.; Han, X.; Bai, T.; Liu, S.; Li, Y.; Jiang, S. Differences in Cationic and Anionic Charge Densities Dictate Zwitterionic Associations and Stimuli Responses. *J. Phys. Chem. B* **2014**, *118*, 6956–6962.

(44) Shao, Q.; Jiang, S. Molecular Understanding and Design of Zwitterionic Materials. *Adv. Mater.* **2015**, *27*, 15–26.

(45) Bengani-Lutz, P.; Converse, E.; Cebe, P.; Asatekin, A. Self-Assembling Zwitterionic Copolymers as Membrane Selective Layers with Excellent Fouling Resistance: Effect of Zwitterion Chemistry. *ACS Appl. Mater. Interfaces* **2017**, *9*, 20859–20872.

(46) Zhang, Z.; Chao, T.; Chen, S.; Jiang, S. Superlow Fouling Sulfobetaine and Carboxybetaine Polymers on Glass Slides. *Langmuir* **2006**, *22*, 10072–10077.

(47) Chintapalli, M.; Timachova, K.; Olson, K. R.; Mecham, S. J.; Devaux, D.; Desimone, J. M.; Balsara, N. P. Relationship between Conductivity, Ion Diffusion, and Transference Number in Perfluoropolyether Electrolytes. *Macromolecules* **2016**, *49*, 3508–3515.

(48) Timachova, K.; Watanabe, H.; Balsara, N. P. Effect of Molecular Weight and Salt Concentration on Ion Transport and the Transference Number in Polymer Electrolytes.

Macromolecules **2015**, *48*, 7882–7888.

(49) Hayamizu, K.; Akiba, E.; Bando, T.; Aihara, Y. 1H, 7Li, and 19F Nuclear Magnetic Resonance and Ionic Conductivity Studies for Liquid Electrolytes Composed of Glymes and Polyetheneglycol Dimethyl Ethers of CH3O(CH2CH2O)NCH3 (n = 3 - 50) Doped with LiN(SO2CF3)2. *J. Chem. Phys.* **2002**, *117*, 5929–5939.

(50) Evans, J.; Vincent, C. A.; Bruce, P. G. Electrochemical Measurement of Transference Numbers in Polymer Electrolytes. *Polymer* **1987**, *28*, 2324–2328.

(51) Bruce, P. G.; Hardgrave, M. T.; Vincent, C. A. Steady State Current Flow in Solid Binary Electrolyte Cells Part 2. The Effect of Ion Association. *J. Electroanal. Chem.* **1989**, *271*, 27–34.

(52) Tiyapiboonchaiya, C.; Pringle, J. M.; Sun, J.; Byrne, N.; Howlett, P. C.; MacFarlane, D. R.; Forsyth, M. The Zwitterion Effect in High-Conductivity Polyelectrolyte Materials. *Nat. Mater.* **2004**, *3*, 29–32.

(53) Yoshizawa, M.; Hirao, M.; Ito-Akita, K.; Ohno, H. Ion Conduction in Zwitterionic-Type Molten Salts and Their Polymers. *J. Mater. Chem.* **2001**, *11*, 1057-1062.

(54) Andrzejewska, E. Photoinitiated Polymerization in Ionic Liquids and Its Application. *Polym. Int.* **2017**, *66*, 366–381.

(55) Kubisa, P. Application of Ionic Liquids as Solvents for Polymerization Processes. *Prog. Polym. Sci.* **2004**, *29*, 3–12.

(56) Kubisa, P. Ionic Liquids as Solvents for Polymerization Processes-Progress and Challenges. *Prog. Polym. Sci.* **2009**, *34*, 1333–1347.

(57) Kido, R.; Ueno, K.; Iwata, K.; Kitazawa, Y.; Imaizumi, S.; Mandai, T.; Dokko, K.; Watanabe, M. Li+ Ion Transport in Polymer Electrolytes Based on a Glyme-Li Salt Solvate Ionic Liquid. *Electrochim. Acta* **2015**, *175*, 5–12.

(58) Ueno, K.; Murai, J.; Ikeda, K.; Tsuzuki, S.; Tsuchiya, M.; Tatara, R.; Mandai, T.; Umebayashi, Y.; Dokko, K.; Watanabe, M. Li+ Solvation and Ionic Transport in Lithium Solvate Ionic Liquids Diluted by Molecular Solvents. *J. Phys. Chem. C* **2016**, *120*, 15792–15802.

(59) Doyle, M.; Fuller, T. F.; Newman, J. The Importance of the Lithium Ion Transference Number in Lithium/Polymer Cells. *Electrochim. Acta* **1994**, *39*, 2073–2081.

(60) Fernicola, A.; Croce, F.; Scrosati, B.; Watanabe, T.; Ohno, H. LiTFSI-BEPyTFSI as an Improved Ionic Liquid Electrolyte for Rechargeable Lithium Batteries. *J. Power Sources* **2007**, *174*, 342–348.

(61) Popovic, J.; Höfler, D.; Melchior, J. P.; Münchinger, A.; List, B.; Maier, J. High Lithium Transference Number Electrolytes Containing Tetratriflylpropene's Lithium Salt. *J. Phys. Chem. Lett.* **2018**, *9*, 5116–5120.

(62) Ueno, K.; Tatara, R.; Tsuzuki, S.; Saito, S.; Doi, H.; Yoshida, K.; Mandai, T.; Matsugami, M.; Umebayashi, Y.; Dokko, K.; Watanabe, M. Li+ Solvation in Glyme-Li Salt Solvate Ionic Liquids. *Phys. Chem. Chem. Phys.* **2015**, *17*, 8248–8257.

TOC Image

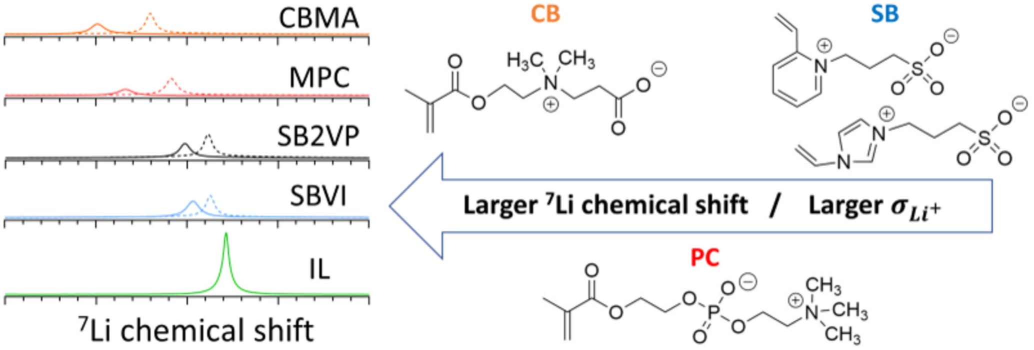
CBMA
MPC
SB2VP
SBVI
IL
^{7}Li chemical shift
CB
SB
PC
Larger ^{7}Li chemical shift / Larger σ_{Li^+}